Computer Assisted Mechanics and Engineering Sciences, 14: 159–166, 2007.

Cracking and failure estimation of reinforced concrete beams on the basis of dynamic characteristics

Lidia Buda-Ożóg, Władysław Łakota
Department of Structural Mechanics
Rzeszów University of Technology, Rzeszów, Poland

(Received in the final form April 23, 2007)

The paper discusses methods of diagnosing the technical condition of reinforced concrete beams, based on the change in dynamic characteristics. The objects of research were 12 reinforced concrete (RC) beams. Testing of RC beams included both static and dynamic tests. A series of step loaded static tests was aimed to produce successive damage to the beams. After each load step (at the moment of displacement and strain stabilization), dynamic testing followed. To carry out the concept of concrete beams diagnosis, on the basis of frequency changes, Artificial Neural Networks (ANNs) were applied.

Keywords: estimation, reinforced concrete beam, dynamics, artificial neural networks

1. Introduction

Accurate estimation of the technical condition of a structure is a basis for its safe use or reinforcement. That is why the development of non-destructive methods of diagnosing of the state of structure elements and building materials has been the subject of a large number of research works in recent years.

The methods are particularly useful for diagnosing engineering constructions of particular importance, such as bridges, all kinds of containers, floating platforms, etc. where the occurrence of even the slightest damage is decisive of further operation. There are a few methods of detecting the damages of a structure. Visual inspection has been and still is the most common method used in detecting damage of a structure. However, conventional visual inspection can be costly and time consuming, especially when disassembly is necessary to provide access to the area under inspection. Non-destructive damage detection techniques such as ultrasonic, acoustic emission, x-ray inspection, etc. are "local" inspection approaches. Structural damage identification through changes in dynamic characteristics provides a "global" way to evaluate the structural state [5]. Therefore dynamics-based damage identification methods have been the subject of a considerable number of research projects in recent years (Deobeling 1996 [1], Vestroni and Capecchi 1996 [6, 7], Ren and De Roeck 1998 [3, 5]).

The extent of neural networks application in structure is increasing. Neural networks are used for identification, designing and optimisation of structures. The network can also be applied as a detector of the difference between signals from damaged and undamaged structures. The article discusses methods of diagnosing the technical condition of reinforced concrete beams, based on the change in dynamic characteristics and the application of ANNs to damage identification.

Reinforced concrete (RC) beams were subjected to an increasing static load to produce successive damage. In those beams strains, displacements, crack location and lengths were measured. After each stage of static loading, dynamic testing followed, with the purpose of determining changes in dynamic characteristics.

2. Description of test beams

The objects of research were 12 reinforced beams. There are three 12 mm diameter steel bars at the bottom of the beam, two 12 mm diameter steel bars at the top of the beam section and stirrup 5.5 mm diameter. Yield strength of the steel bar is: 240 MPa for stirrups and 410 MPa for main bars. The dimensions and reinforcement of the beams are shown in Fig. 1.

These beams were made in stages, two at a time. Each time the beams were made of the same class and recipe concrete. The properties of concrete: characteristic compressive strength of concrete (f_{ck}) at 28 days and density (ρ) for each beam are shown Table 1.

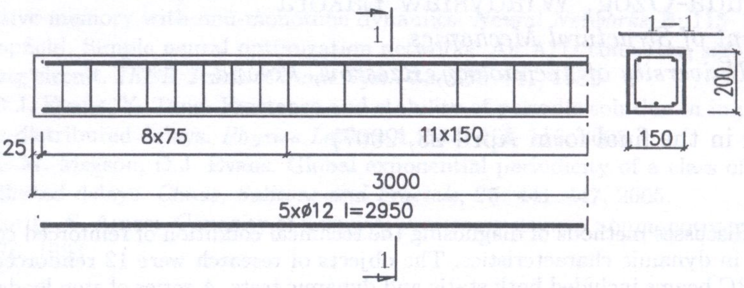

Fig. 1. Dimensions and reinforcement of beams

Table 1. Characteristic compressive strength of concrete and density for twelve beams

Number of beam	f_{ck} [MPa]	ρ [kg/m^3]
B1, B2	30.3	2187
B3, B4	30.0	2197
B5, B6	31.0	2211
B7, B8	30.1	2328
B9, B10	32.0	2264
B11, B12	29.7	2237

3. Test setup

Testing of reinforced concrete beams included both static and dynamic tests. A series of step loaded static tests were aimed at producing successive damage to the beams. After each static load step (at the moment of displacement and strain stabilization), dynamic testing followed. Consequently, the dynamic characteristics of the test beams can be obtained for the reference state and each successive damage state.

3.1. Static testing

In the setup of static testing, the beam was simply supported at both sides with a cantilever of 0.1 m. The beam was loaded by two symmetric point loads at a distance of 1 m (four-point bending). The static test configuration is shown in Fig. 2. Load was made by the steps from 1 kN to failure of beam. Failure of beams were observed for load from 62 kN to 72 kN depending on beam. While each load steps, displacements, strain, crack location and lengths were measured. After loading, at the moment of displacement and strain stabilization, the cracks were measured again.

On the basis of the theory of flexure of reinforced concrete beam [2], describing the behaviour of a beam cross section under increasing moment, four damage states were introduced:

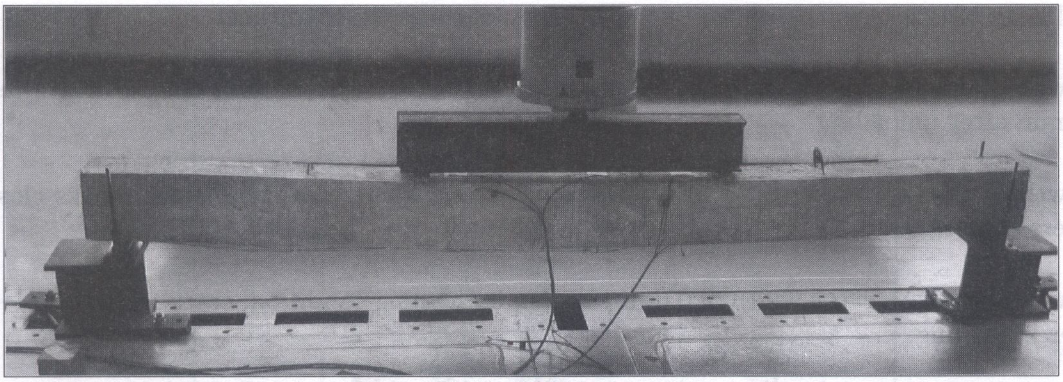

Fig. 2. Static test setup

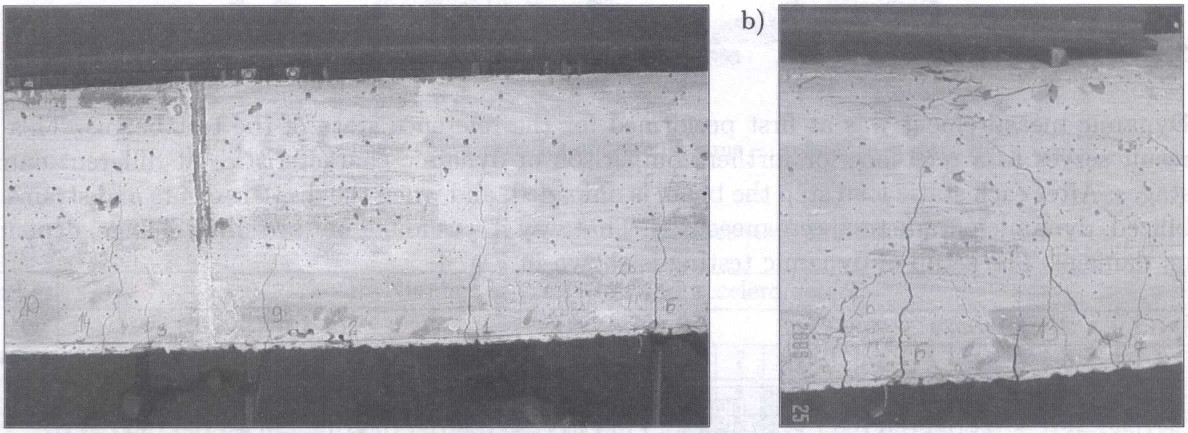

Fig. 3. Crack pattern and damage: a) state 2, b) state 4, failure of the beam

1. no cracking was observed, the strains at this stage were very small, the stress distribution was linear.
2. the stresses at the bottom of the beam cross-section reached the concrete tensile strength, cracking occurred. After cracking, the tensile force in the concrete was transferred to the steel. In the compression zone the stress distribution was linear. In this damage state cracks width of 0.1–0.3 mm under loading condition were observed. After unloading cracks width less than 0.1 mm were visible.
3. as the load was increased, the stress distribution in the compression zone became more markedly non-linear. This stage was observed, when some cracks closed while others were increased rapidly. For this damage state cracks width of 0.5–1.0 mm under loading condition were observed and 0.1–0.2 mm after unloading.
4. failure of the beam, cracks width above 1.0 mm, evolution of cracks to compression zone with simultaneous crushing of concrete of the compression face.

Figure 3 shows the crack pattern and damage for states number 2 and 4.

Then, on the basis of crack location and lengths measured during load and unload steps, the number of damage states were multiplied and eight damage states were introduced:

1. no visible cracking,
2. the first small, single crack at midspan, crack width of < 0.1 mm under loading condition,
3. further cracks near midspan locations, crack width of 0.1–0.2 mm under loading condition,

4. evolution of cracks to the centre line of beam under loading condition,

5. growth of cracks, cracks width of 0.2–0.3 mm under loading condition, cracks width less than 0.1 mm after unloading,

6. growth of cracks, cracks width of 0.5–0.6 mm under loading condition, some cracks close while others evolve,

7. growth of cracks, cracks width of 0.6–1.0 mm under loading condition, crack width of 0.1–0.2 mm after unloading,

8. failure of the beam, cracks width above than 1.0 mm, evolution of cracks to compression zone.

3.2. Dynamic testing

Dynamic measurement was at first performed for the reference state of the test beams. This test result serves as a reference for further comparison of dynamic characteristics at different damage stages. After each static load step the beam is unloaded, and when the displacements and strains stabilized, dynamic parameters were measured. That way it was found out how they change, depending on damage. The setup of dynamic testing is shown in Fig. 4.

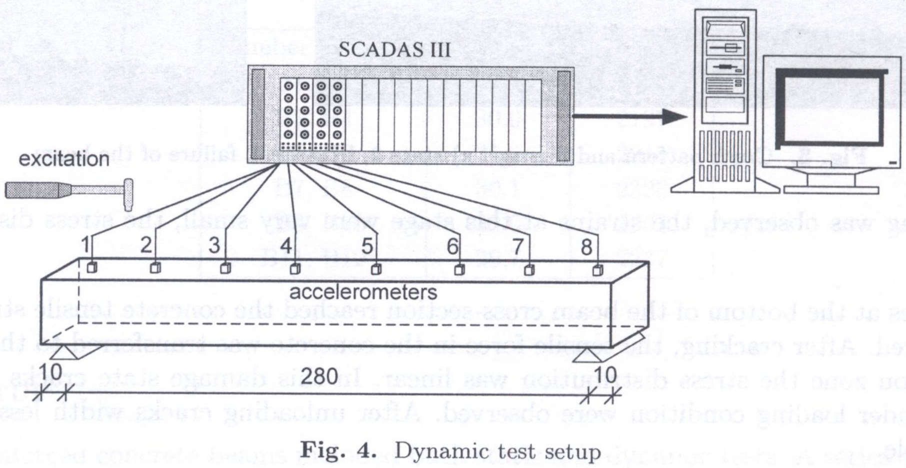

Fig. 4. Dynamic test setup

During dynamic testing each beam was excited by means of an impact hammer at three independent points on the beam. The response of beams to the impulse excitation was recorded by eight accelerometers. The data signal from each accelerometer was recorded by SCADAS III instrumentation recorder and it was processed by means of LMS CADA-X software from LMS Incorporated.

Frequency characteristics for each beam at each load step were obtained. Frequency characteristics of RC beams for the reference state are shown in Fig. 5. The natural frequencies are identified visually via the amplitude peaks of the frequency spectrum.

The first five identified frequencies of the test beams were selected from the whole range of frequency characteristics measured from 0 Hz to 500 Hz. Table 2 shows resonance frequencies measured for the reference state of beam B1.

The change of mean ± standard deviation of the first resonance frequencies for all the 12 tested beams, depending on the load step, are shown in Table 3.

The mean ± standard deviation of the relative changes of frequencies with respect to the reference state (undamaged state) for five identified frequencies and damage states (four and eight) are

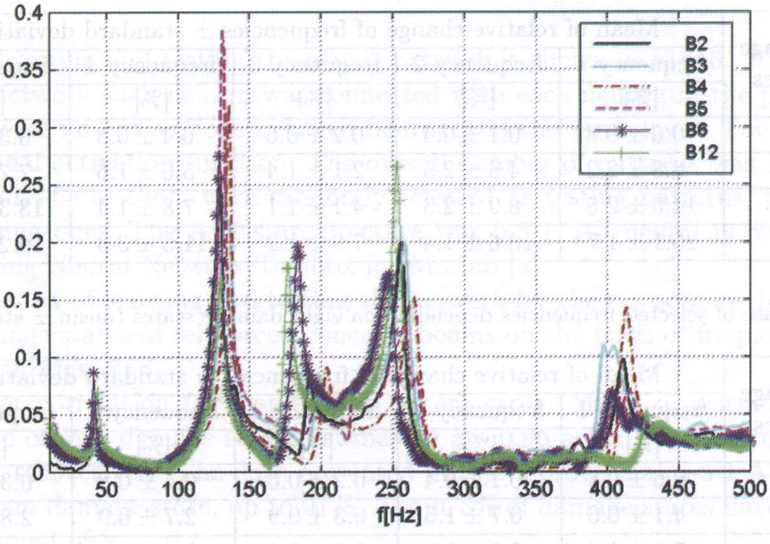

Fig. 5. Frequency characteristics of tested beams — reference state

Table 2. Identified frequencies for the reference state of beam B1

Number of frequencies	Number of excitation and accelerometers																							
	excitation 1								excitation 2								excitation 3							
	1	2	3	4	5	6	7	8	1	2	3	4	5	6	7	8	1	2	3	4	5	6	7	8
1	*	42	43	42	42	42	*	*	*	42	42	42	41	42	*	*	*	43	42	42	42	42	*	*
2	133	134	135	135	*	*	135	135	135	134	135	134	*	135	134	135	135	135	135	134	*	135	135	135
3	189	*	189	186	186	187	*	186	189	187	*	187	188	188	*	187	187	187	*	187	188	187	*	187
4	240	236	239	239	242	240	240	240	240	235	241	241	237	241	241	241	235	236	235	235	237	235	235	235
5	411	406	410	408	409	410	409	409	407	407	407	407	407	407	406	405	406	407	406	406	406	408	406	405

* – frequency was not measured

Table 3. Mean ± standard deviation of the first resonance frequencies for 12 tested beams

Number of beams	Load steps						
	0 kN	6 kN	12 kN	24 kN	40 kN	60 kN	the last load step (62÷72 kN)
	[Hz]	[Hz]	[Hz]	[Hz]	[Hz]	[Hz]	[Hz]
B1	42 ± 0.5	41 ± 0.0	38 ± 0.5	37 ± 0.5	37 ± 0.5	37 ± 0.3	31 ± 0.3
B2	41 ± 0.5	41 ± 0.5	39 ± 0.0	37 ± 0.0	37 ± 0.5	36 ± 0.5	31 ± 0.5
B3	41 ± 0.3	40 ± 0.0	38 ± 0.3	37 ± 0.5	37 ± 0.5	36 ± 0.5	34 ± 0.5
B4	42 ± 0.4	42 ± 0.5	39 ± 0.5	38 ± 0.3	38 ± 0.5	37 ± 0.3	32 ± 0.5
B5	41 ± 0.5	40 ± 0.4	38 ± 0.3	37 ± 0.0	37 ± 0.3	36 ± 0.5	30 ± 0.4
B6	41 ± 0.0	41 ± 0.5	39 ± 0.5	37 ± 0.3	37 ± 0.5	35 ± 0.5	32 ± 0.4
B7	41 ± 0.6	41 ± 0.3	39 ± 0.4	38 ± 0.0	38 ± 0.0	37 ± 0.5	36 ± 0.3
B8	40 ± 0.3	39 ± 0.3	38 ± 0.5	37 ± 0.5	37 ± 0.5	37 ± 0.4	34 ± 0.4
B9	42 ± 0.6	42 ± 0.3	41 ± 0.5	39 ± 0.4	39 ± 0.4	39 ± 0.3	36 ± 0.3
B10	44 ± 0.3	44 ± 0.3	43 ± 0.3	42 ± 0.4	40 ± 1.5	38 ± 1.5	35 ± 0.0
B11	43 ± 0.5	42 ± 0.6	41 ± 0.0	39 ± 0.5	39 ± 0.4	38 ± 0.4	31 ± 1.3
B12	44 ± 0.4	43 ± 0.3	42 ± 0.0	40 ± 0.6	40 ± 0.5	39 ± 0.3	36 ± 0.3

Table 4. Decrease of selected frequencies depending on four damage states (mean ± standard deviation)

Damage states	Mean of relative change of frequencies ± standard deviation				
	frequency 1 [%]	frequency 2 [%]	frequency 3 [%]	frequency 4 [%]	frequency 5 [%]
1	0.6 ± 0.8	0.1 ± 0.4	0.2 ± 0.6	0.4 ± 0.8	0.3 ± 0.5
2	8.8 ± 2.2	4.8 ± 2.5	2.1 ± 1.4	5.0 ± 1.6	7.7 ± 2.6
3	14.5 ± 2.5	8.9 ± 2.3	4.1 ± 1.1	7.8 ± 1.4	13.3 ± 2.1
4	25.1 ± 1.7	13.6 ± 1.4	7.9 ± 1.2	11.3 ± 3.3	19.2 ± 2.5

Table 5. Decrease of selected frequencies depending on eight damage states (mean ± standard deviation)

Damage states	Mean of relative change of frequencies ± standard deviation				
	frequency 1 [%]	frequency 2 [%]	frequency 3 [%]	frequency 4 [%]	frequency 5 [%]
1	0.6 ± 0.8	0.1 ± 0.4	0.2 ± 0.6	0.4 ± 0.8	0.3 ± 0.5
2	4.1 ± 0.6	0.7 ± 1.6	0.3 ± 0.9	2.7 ± 0.9	2.8 ± 0.6
3	7.1 ± 1.4	2.9 ± 1.3	1.4 ± 0.9	3.7 ± 1.4	5.1 ± 1.0
4	8.6 ± 1.4	4.5 ± 1.4	2.0 ± 1.2	4.9 ± 1.1	7.3 ± 0.9
5	10.0 ± 1.5	6.0 ± 2.2	2.6 ± 1.4	5.9 ± 1.1	9.5 ± 1.5
6	13.4 ± 1.8	9.3 ± 1.5	4.0 ± 1.1	7.4 ± 1.2	12.6 ± 2.2
7	16.4 ± 2.6	8.3 ± 3.3	4.2 ± 1.1	8.7 ± 1.4	14.6 ± 1.1
8	25.2 ± 1.7	13.6 ± 1.4	7.9 ± 1.2	11.3 ± 3.3	19.2 ± 2.5

summarized in Tables 4 and 5, respectively. The relative frequency changes of resonance frequencies given in this table were calculated from Eq. (1),

$$\Delta f_{(i)}^{k} = \frac{f_{r(i)} - f_{d(i)}^{k}}{f_{r(i)}} * 100\% \,, \tag{1}$$

where $f_{r(i)}$ — reference resonance frequency, $f_{d(i)}^{k}$ — resonance frequency after damage, i — number of frequencies, and k — number of damage states.

In order to compare mean values of the decrease of selected frequencies for four and eight damage states, a test of analysis variance was carried out. This test proved that division for eight damage states was too detailed. The hypothesis about equality of mean values was not rejected, for the level of significance $p < 0.05$, for 3,4,5 and 6,7 damage states.

For the five identified frequencies, mode shapes were determined. It can be observed that the damage does influence the mode shapes.

4. Artificial neural networks in concrete beam estimation

Taking advantage of the research presented in the literature [8], error back-propagation neural networks, for estimating the damage states of RC beams based on the change in the selected resonance frequencies were built. To carry out the concept of the diagnosis, multi-layer feed-forward ANN consisting of the following layers was applied:

- input layer made up of 5 neurons. The input vector consisted of independent changes in the selected resonance frequencies as a result of the damage states,

  $\mathbf{x}_{(5\times1)} = \{\Delta f_1\,, \Delta f_2\,, \Delta f_3\,, \Delta f_4\,, \Delta f_5\}^T,$

- one hidden layer of experimentally determined size, based on the number of inputs, outputs and patterns,

- output layer made up of one neuron. The output vector consisted of damage states of RC beam, $\mathbf{y}_{(1\times1)} = \{D\}$.

The scheme of learning and testing the neural network is shown in Fig. 6.

In the applied network each neuron was connected with each neuron in the previous and in the next layer. There were no connections between neurones in the same layer. The neurons that were used, had a sigmoidal activation function. The overall number of patterns was 159 (12 beams and 12÷14 steps of load), 64 of them were randomly selected as testing patterns, the remaining ones were used as learning ones. The ANNs architecture was 5-5-1. All neural networks computations were performed using Neural Network Toolbox for Matlab [4].

The obtained results of learning and testing the network for the purpose of the estimation of the four and eight damage states of reinforced concrete beams on the basis of frequencies changes were graphically shown in Figs. 7, 8.

The linear factor correlation (R^2) and mean square error (MSE) of learning of the proposed network in the case of four damage stages estimation are 0.96 and 0.021, whereas for testing they are 0.96 and 0.031, respectively. The data presented in Fig. 8 prove that 5-5-1 ANNs are capable of identifying four beam damage state, up to 97%. About 3% of damage states have been identified as 2 damage state instead of 3.

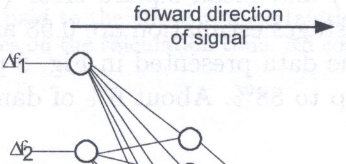

Fig. 6. Artificial Neural Network architecture

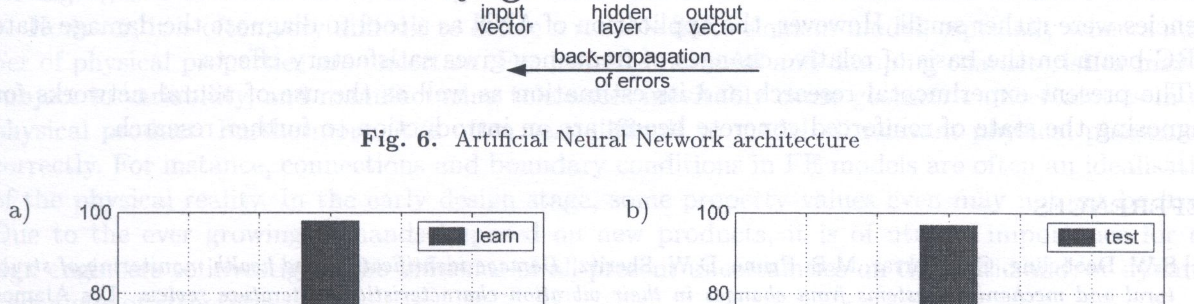

Fig. 7. The results of estimation of four damage states a) learning, b) testing

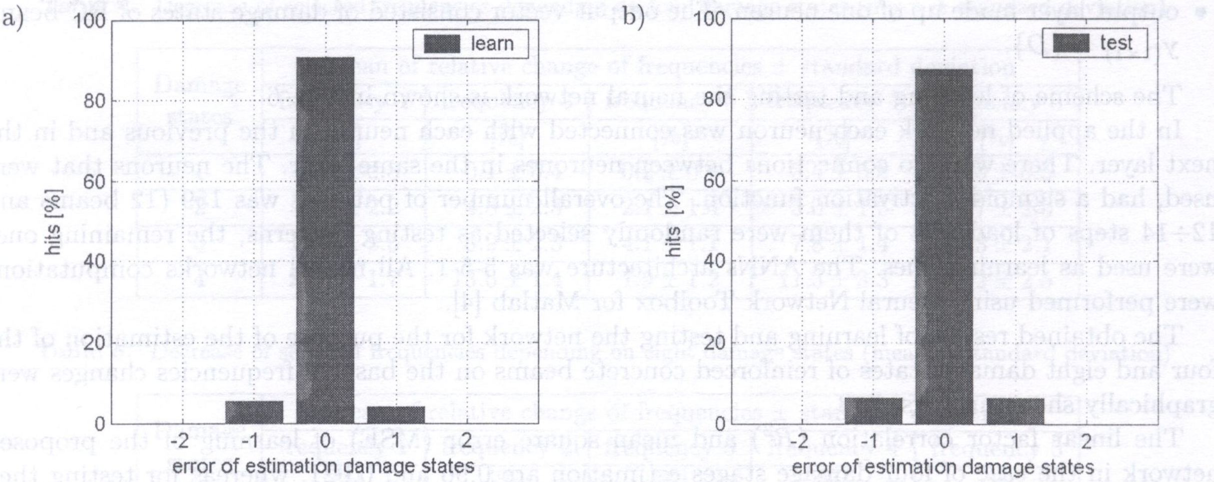

Fig. 8. The results of estimation of eight damage states a) learning, b) testing

The linear factor correlation (R^2) and mean square error (MSE) of learning of the proposed network in the case of eight damage stages estimation are 0.98 and 0.0945, whereas for testing they are 0.973 and 0.125, respectively. The data presented in Fig. 8 prove that 5-5-1 ANNs are capable of identifying beam damage state, up to 88%. About 6% of damage states have been identified as too high and 6% as too low.

5. Final remarks

The present paper describes a procedure of identification of real successive damage through changes in dynamic characteristics of twelve reinforced concrete beams. The obtained relative changes of selected resonance frequencies for those beams are similar. Considerable changes in the resonance frequencies (of RC beams) are observed when the first cracks appear and at the moment of the reinforced concrete beam failure. For the intermediate damage states, the obtained changes of frequencies were rather small. However, the application of ANN as a tool to diagnose the damage state of RC beam on the basis of relative changes of frequency gives satisfactory effects.

The present experimental research and its estimation as well as the use of neural networks for diagnosing the state of reinforced concrete beams are an introduction to further research.

References

[1] S.W. Deobeling, C.R. Farrar, M.B. Prime, D.W. Sheritz. *Damage identification and health monitoring of structural and mechanical systems from changes in their vibration characteristic: a literature review.* Los Alamos Natl. Lab, 1996.

[2] J.G. MacGregor, J.K. Wight. *Reinforced Concrete, Mechanics and Design.* Pearson Prentice Hall, New Jersey, 2005.

[3] J. Maeck, M. Abdel Wahab, G. De Roeck. Damage detection in reinforced concrete structures by dynamic system identification. *Proceedings ISMA 23, Noise and Vibration Engineering*, Leuven, Belgium, **9**: 939–946, 1998.

[4] *Neural Network Toolbox for Use with Matlab, User's Guide, Version 3.0.* The MathWorks, Inc.

[5] W. Ren, G. De Roeck. Structural damage identification using modal data. *Journal of Structural Engineering*, **1**: 87–104, 2002.

[6] B.F. Vestroni, D. Capecchi. Damage evaluation in cracked vibrating beams using experimental frequencies and finite element models. *Journal of Vibration and Control*, **2**: 69–86, 1996.

[7] B.F. Vestroni, D. Capecchi. Damage detection in beam structures based on frequency measurements. *Journal of Engineering Mechanics*, **7**: 761–768, 2000.

[8] Z. Waszczyszyn, L. Ziemiański. Neural networks in mechanics of structures and materials — new results and prospect of applications. *Computers and Structures*, **79**: 2261–2276, 2001.